19

Periodically perforated aluminum film for enhancing chemiluminescence

© N.S. Petrov, D.R. Dadadzhanov, T.A. Vartanyan

ITMO University,
St. Petersburg, Russia

e-mail: Tigran.Vartanyan@mail.ru

Received November 15, 2024
Revised November 15, 2024
Accepted December 03, 2024

The influence of a thin periodically perforated aluminum film on the rate of radiative relaxation of excited luminol molecules was investigated. Numerical modeling showed that an aluminum film with a thickness of 20 nm and cylindrical holes with a radius of 36 nm, arranged in a square lattice with a period of 230 nm, accelerates the chemiluminescence of luminol at a wavelength of 430 nm. The acceleration of radiative transitions and the corresponding increase in chemiluminescence intensity exceed 10 times in most of the volume of the nanohole and are weakly dependent on the position of the emitting molecule and the orientation of the transition dipole moment.

Keywords: radiative transitions, chemiluminescence, plasmon resonance, luminol.

DOI: 10.61011/EOS.2025.01.60572.7341-24

Introduction

The study of phenomena caused by chemiluminescence is one of the promising areas of research and development related to chemical and biological sensors. Chemiluminescent sensors, the operation principle of which is based on light emission from chemiluminophore molecules excited as a result of a chemical reaction, are featuring high sensitivity and selectivity, which attracts interest to them in the scientific community. Due to their unique parameters, chemiluminescent sensors have found application in medical diagnostics [1], pharmaceuticals [2] and detection of reactive oxygen species (ROS) [3,4]. The undisputable advantage of chemiluminescent sensors is the absence of an external radiation source, the need for which in all other optical sensors leads to an increase in their size, cost and other limitations. At the same time, the intrinsic radiation of the chemiluminophore in many cases turns out to be too weak to be reliably detected by simple optical radiation receivers. The problem becomes especially acute at low concentrations and limited amounts of the substances studied. To solve it, two different methods can be used: increasing the sensitivity of radiation detectors or increasing the intensity of chemiluminescence. In this paper, the possibility of enhancing the intensity of chemiluminescence using plasmonic nanostructures is investigated.

One of the available methods of increasing the intensity of radiation during chemiluminescence is the use of metal structures with plasmon resonance. Due to the Purcell effect, the radiation decay of chemiluminophores is significantly accelerated, which leads to an increase in the quantum yield of chemiluminescence [5–7]. Various types of structures with plasmonic properties are suitable for implementation of this method: from colloidal solutions of nanoparticles to thin nanostructured films. Each type of the plasmonic structures has its own benefits and shortcomings. For example, when using colloidal nanoparticles, the results are poorly reproduced due to the significant effect of dispersion in particles size and shape: with a sufficiently large spread in size and shape, most of the nanoparticles leave resonance with chemiluminescent molecules, thus, resulting in lower emission enhancement [8]. To achieve a more specific and reproducible result, instead of a colloidal solution of nanoparticles, thin nanostructured metal films can be used, which also have plasmon resonances, which similarly affect the quantum yield of luminescence. The major drawback of this approach is lower area of contact between the metal and luminophore. But, in turn, the formation of such surfaces is associated with much smaller inaccuracies, which means that the experimental results will be reproduced with greater accuracy. Moreover, the fabrication of such metasurfaces can employ a range of technologies, from chemical etching [9,10] to lithographic methods [11,12]. These techniques are inherently scalable a critical advantage for enabling the commercial deployment of sensors based on these structures.

Description of material and structural parameters of a perforated film

In this paper, a periodic structure consisting of a thin (5−40 nm) aluminum film with sub-wavelength cylindrical holes is investigated. The choice of this particular type of metasurface is determined by a number of critical material and structural parameters. Firstly, despite the fact that plasma frequency of aluminum is in the ultraviolet region of the spectrum, the plasmon resonance of a nanostructured aluminum film can be shifted to visible region provided its parameters were appropriately selected. Secondly, the high chemical resistance of aluminum, due to the presence of a natural oxide film, allows it to be used in an aqueous

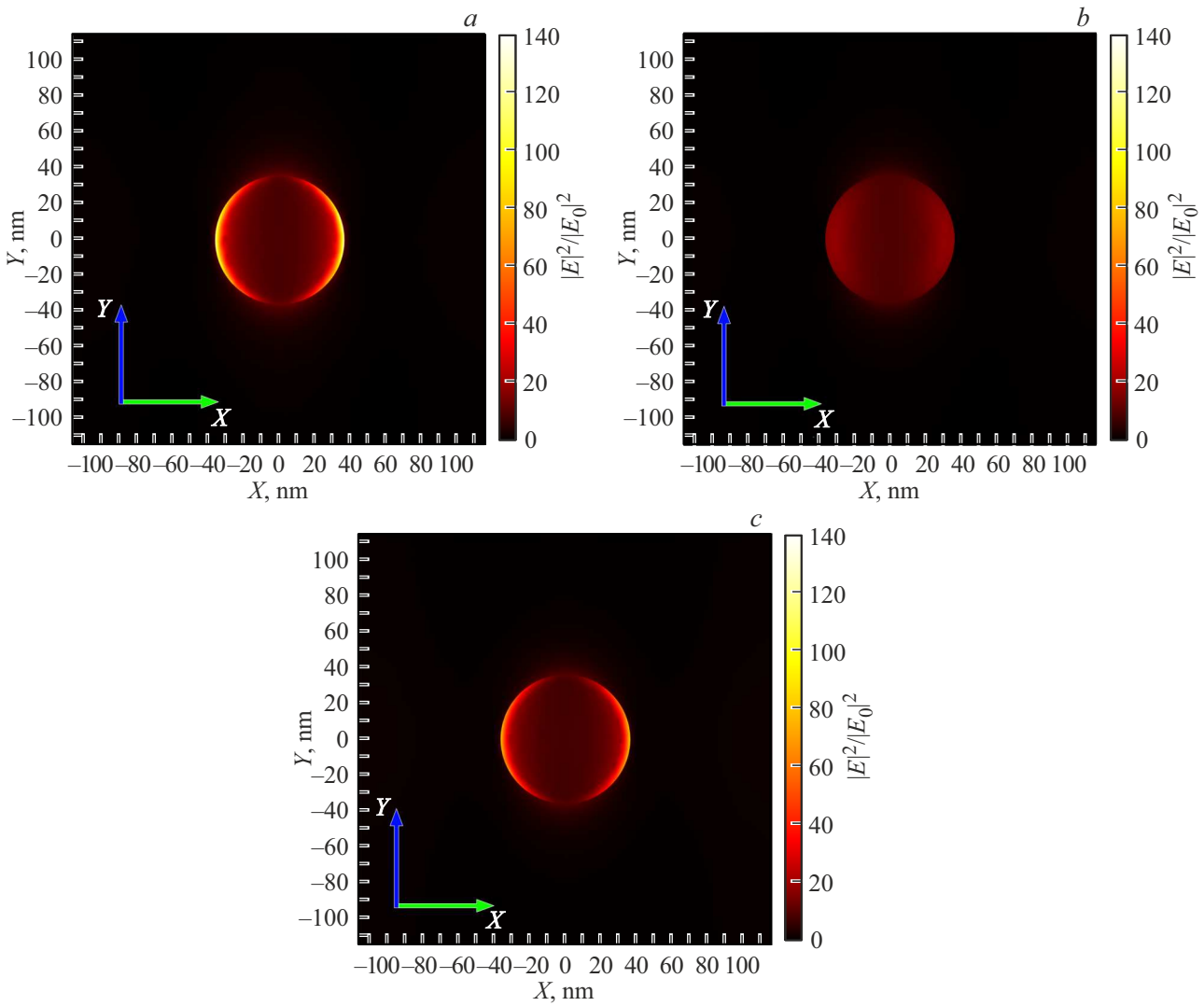

Figure 1. Distribution of local field enhancement $|E|^2/|E_0|^2$ within the unit cell of a square lattice with a period of 230 nm, consisting of a 20 nm thick aluminum film with cylindrical holes with a radius of 36 nm. The field enhancement maps are plotted with distances from the quartz substrate 0 (*a*), 10 nm (*b*) and 20 nm (*c*). Incident radiation at a wavelength of 430 nm, corresponding to the maximum of the luminol chemiluminescence band, is linearly polarized along the *x* axis.

environment. Thirdly, aluminum is a much more affordable and cheaper material than silver and gold widely used in plasmonics, the cost of which outpaces the cost of aluminum by 400 and 30,000 times, respectively. Fourth, fabricating metasurfaces from a solid film requires removing only the material at the hole site, whereas producing nanocylinder-based metasurfaces demands the removal of most surrounding material significantly increasing complexity, fabrication precision requirements, and production time. And finally, fifthly, as follows from computations performed and shown in Fig.1, when a plane electromagnetic wave falls on the structure inside cylindrical holes, the field enhancement is relatively uniform, which gives reason to hope that acceleration of radiation transitions inside the entire volume of the hole will not change as much as in the space between cylindrical projections examined earlier [6,7].

The optimization of nanoscale cylindrical hole dimensions and lattice period to ensure alignment between plasmon resonance and the luminol chemiluminescence emission band was conducted across square lattice configurations with periods systematically varied from 220 to 250 nm. Aluminum, which has favorable plasmonic properties in the visible part of the spectrum, was chosen as the material of the film, the thickness of which varied from 5 to 40 nm, provided that a suitable nanostructure was formed. Nanostructures composed of circular cylindrical holes with radii systematically varied from 10 to 60 nm were investigated. It was assumed that the aluminum film with holes should be located on a quartz substrate with a refractive index of 1.46. The dispersion of the substrate's refractive index was neglected. In accordance with the intended conditions of use, it was assumed that

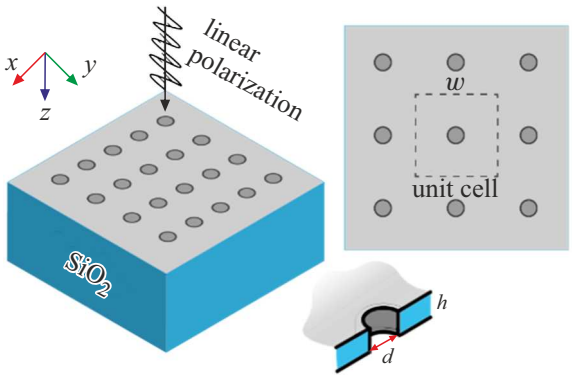

Figure 2. Arrangement of cylindrical holes in the quartz substrate aluminum film. The holes form a square lattice. In the model, the pores were assumed to be fully saturated with the target medium, with its refractive index set equivalent to that of water.

the system was immersed in an aqueous solution of anolyte and luminol. Due to the low concentrations of the latter, the difference between the refractive index of the environment and the refractive index of water — 1.33 — was neglected. The optical properties of aluminum were taken from [13].

The optical properties of this metasurface were studied using COMSOL Multiphysics® software package. Using the finite element method and Floquet boundary conditions, the field distributions near a metal film with cylindrical holes and the reflection spectra (R) and transmission spectra (T) of incident radiation were calculated. Absorption spectra (A) were calculated by formula $A = 1 - T - R$. During optimization process, it was assumed that maximum amplification of chemiluminescence would be provided by the structure with the highest absorption at a wavelength of 430 nm, corresponding to the maximum of luminol chemiluminescence band. The geometric parameters of the model used in the calculations are shown in Fig. 2.

Absorption spectra of perforated aluminum film

As a starting point to begin the improvement process the parameters of previously calculated optimal inverted nanostructure consisting of circular cylinders were taken, namely: the structure period of 250 nm, the cylinders height of 20 nm, the radius of 35 nm [7].

At the first stage of modelling, the dependence of the absorption spectra of a perforated aluminum film on the period of lattice (with cylindrical holes in its sites) was studied. As can be seen from Fig. 3, with an increase in the structure period, a monotonous long-wave shift of the maximum of the absorption spectrum is observed, as well as a decrease in the absorption magnitude. Upon computation the period providing the maximum absorption of the structure at the maximum of the luminol chemiluminescence band (430 nm) was determined, which was 230 nm

At the next stage of modelling, the dependence of metasurface absorption spectra on the thickness of the aluminum film was studied. At this stage, the optimal value of the metasurface period was taken into account. As can be seen from Fig. 4, as the thickness of aluminum rises, the absorption peak tends to a wavelength of 390 nm and the absorption band narrows. In addition, it can also be noted that the structure has the highest absorption value at a wavelength of 408 nm with a thickness of 28 nm. The optimal thickness value is 20 nm, since at this thickness the greatest absorption is observed at a wavelength of 430 nm.

At the last stage of modelling, the dependence of the absorption spectra of the metasurface on the radius of cylindrical holes was studied. The optimal lattice period and aluminum layer thickness were both incorporated into the analysis. As can be seen from Fig. 5, the surface with holes with a radius of 36 nm has the highest absorption value at a wavelength of 430 nm. It can also be noted that the metasurface with a hole radius of 50 nm at a wavelength of 458 nm has the highest absorption value at the specified parameters.

Calculation of the radiation-induced transitions acceleration near the perforated aluminum film

The absorption calculation described above was used to pre-select a nanostructure with plasmon resonance in the luminol chemiluminescence band. The suitability of the selected nanostructure for enhancing the chemiluminescence of luminol should be clarified based on the calculation of Purcell factor F_P, which reflects an increase in the rate of radiation transition of the excited chemiluminophore molecule near the nanostructure compared with the same process in a free space.

To find Purcell factor, a point dipole oscillating at the frequency of the radiative transition of the excited molecule is placed at various points of the nanostructure, and the integral intensity of its radiation in the direction away from the nanostructure (Φ_1) is calculated. The obtained value is compared with the intensity of radiation in the same direction in a homogeneous medium (Φ_0). Purcell factor is equal to the ratio of these intensities $F_P = \Phi_1/\Phi_0$. The dependence of the Purcell factor on position inside and near the hole and on orientation of the transition dipole moment in horizontal plane is shown in Fig.6 for the selected nanostructure, which is itself a 20 nm thick aluminum film with through 36 nm radius cylindrical holes located at the sites of a square lattice with a period of 230 nm.

Due to the symmetry of the problem, the Purcell factor on the axis of the cylindrical hole does not depend on the orientation of the dipole moment of transition in horizontal plane. It reaches its maximal value of 16.4 at the hole bottom and gradually goes down to 8.7, when the dipole is located 10 nm higher than the outer surface of the aluminum film. When the radiative molecule is displaced

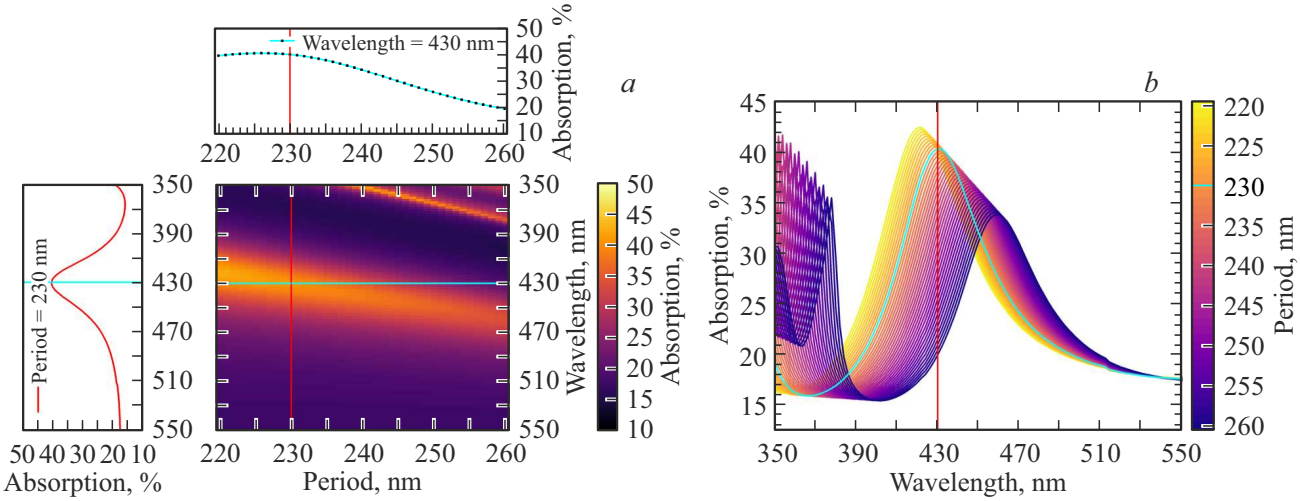

Figure 3. (*a*) Perforated aluminum film versus period structure and wavelength of incident light. The absorption value in percentage is encoded by color. The figure also shows the curve of absorption at a wavelength of 430 nm versus structure period and the absorption spectrum of the metasurface with a period of 230 nm. (*b*) Absorption spectra of a perforated aluminum film depending on the structure period. The figure highlights the absorption spectrum of a metasurface with a period of 230 nm. The color-coded period of the structure in nanometers.

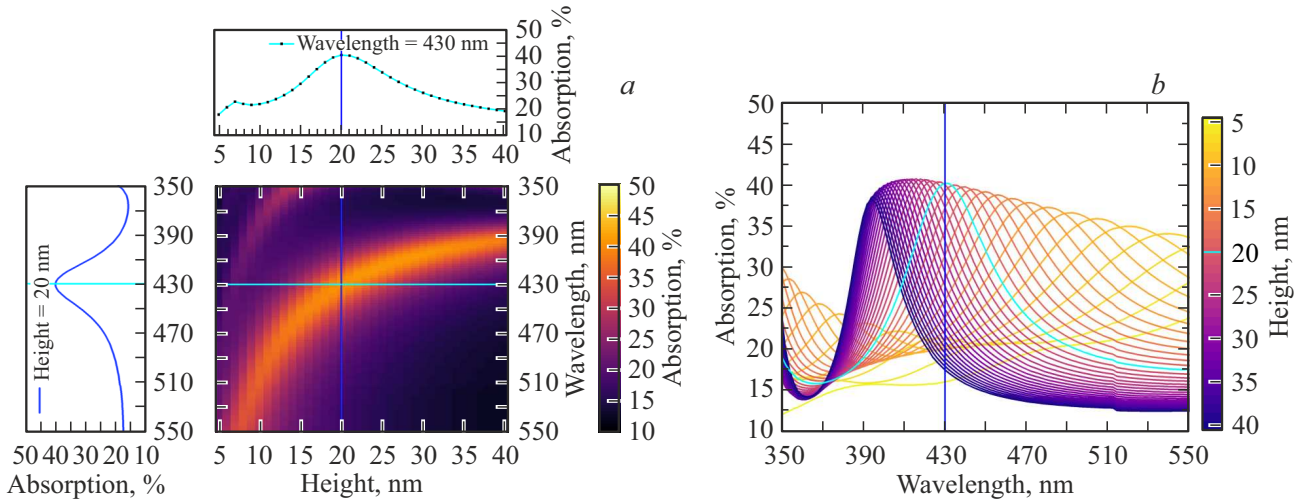

Figure 4. (*a*) Dependence of the Purcell factor on the spatial position and orientation of an emitting molecule within a nanohole. The absorption value in percentage is encoded by color. The figure also shows the curve of absorption at a wavelength of 430 nm versus aluminum layer thickness and the absorption spectrum of the metasurface with a thickness of 20 nm. (*b*) Absorption spectra of a perforated aluminum film depending on thickness. The figure highlights the absorption spectrum of a metasurface with a thickness of 20 nm. The color-coded thickness of the film in nanometers.

from the hole axis, the Purcell factor depends on both, the direction of displacement and the orientation of the transition dipole moment. By restricting the radiating molecule's displacement to the center of the nearest square lattice unit cell, it is sufficient to compute the Purcell factor for two dipole orientations: radial (aligned along the displacement direction) and tangential (parallel to the tangent of the cylindrical hole's cross-section at the closest point on the metal film). With the tangential orientation of the transition dipole moment, its acceleration changes slightly as it moves away from the hole axis. With the radial orientation of the dipole moment of transition, the radiation rate in the main part of the cavity also changes smoothly as it moves away from the hole axis, but increases sharply as the molecule approaches the side surface of the hole in a metal film.

Discussion of the results

As mentioned earlier, many applications of chemiluminescent sensors in biochemistry, medical diagnostics and

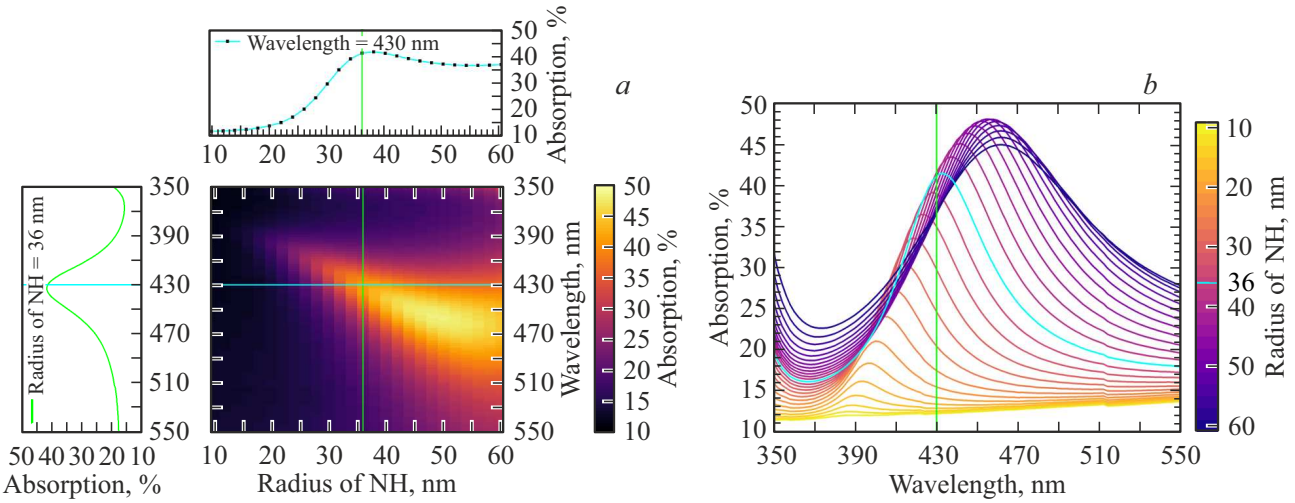

Figure 5. (*a*) Perforated aluminum film absorption versus holes radius and wavelength of incident radiation. The absorption value in percentage is encoded by color. The figure also illustrates the curve of absorption at a wavelength of 430 nm versus holes radius and the absorption spectrum of a metasurface with 36 nm radius holes. (*b*) Absorption spectra of thin aluminum film metasurface with cylindrical holes depending on the radius of the holes. The figure highlights the absorption spectrum of a metasurface with the holes radius of 36 nm. The color-coded holes radius in nanometers.

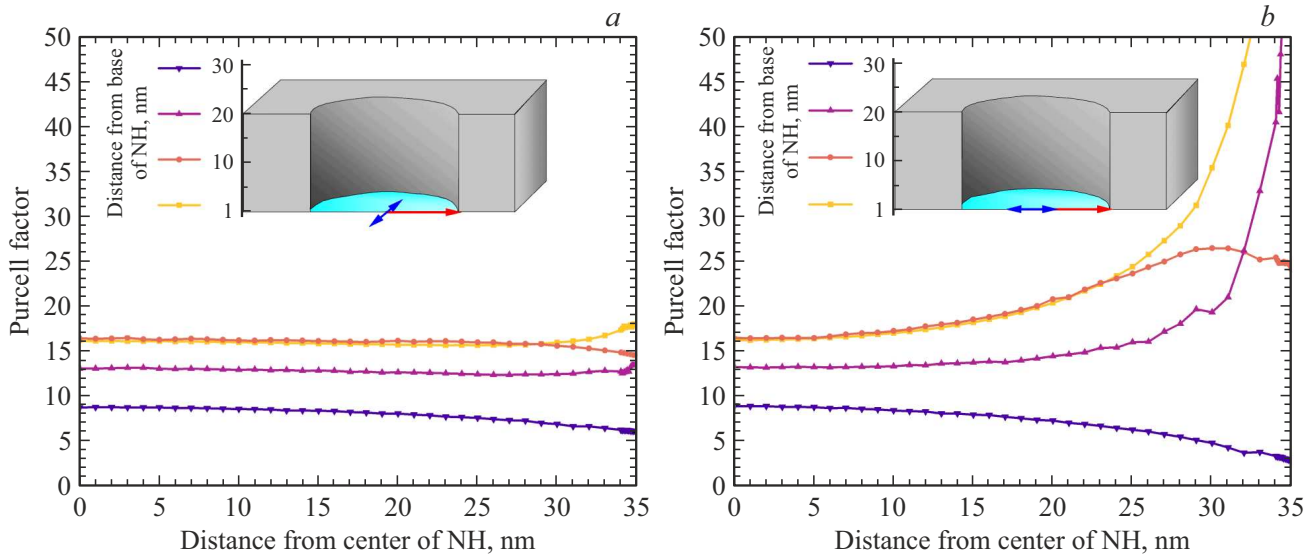

Figure 6. Purcell factor versus position and orientation of the radiating molecule in the nano-hole. The graphs show the change in the rate of radiation transitions as a molecule moves from the center of a given unit cell (center of NH) towards the center of the nearest neighboring unit cell. Orientation of the dipole moment of transition is shown by a blue arrow. The molecule position in height (distance from the base of NH) is shown in color. (*a*) The transition dipole moment is perpendicular to the highlighted direction of the molecule motion (tangential). (*b*) Dipole moment is parallel to the highlighted direction of the molecule motion (radial).

pharmaceuticals industry are based on the process of luminol oxidation by one or another active form of oxygen. It is the oxidation process when the products of chemical reaction in excited state are formed with light emission during transition. Since deactivation of the excited state of chemical reaction products is possible not only by emitting photons, but also in a non-radiative manner, the quantum yield of chemiluminescence QE_0 is determined by the competition of these processes, which can be quantified by the formula

$$QE_0 = \frac{\gamma_{rad}}{\gamma_{rad} + \gamma_{non-rad}}, \qquad (1)$$

where γ_{rad} — rate of radiative transitions, and $\gamma_{non-rad}$ — rate of non-radiative transitions. If, as it often happens, the rate of non-radiative transitions is much higher than the radiative transition rate, the quantum yield of chemiluminescence is small, but can be increased by increasing the rate of radiative transitions.

An increase in the rate of radiative transitions can be achieved by visiting a radiation source near a nano-antenna with resonances at the emitter frequencies [14,15]. In this case, the rate of radiation decay of the molecule changes due to the Purcell effect, and the quantum yield is expressed as

$$QE = \frac{F_P \gamma_{rad}}{F_P \gamma_{rad} + \gamma_{non-rad}}, \quad (2)$$

where F_P — Purcell factor. If a nano-antenna is a structure consisting of materials with plasmonic properties, then, metal-enhanced chemiluminescence is implied [5]. Given that $\gamma_{non-rad}\gamma_{rad} \gg F_P\gamma_{rad}$, the increase of the chemiluminescence quantum yield is approximately equal to the acceleration of radiation-induced transitions:

$$\frac{QE}{QE_0} = F_P \frac{\gamma_{rad} + \gamma_{non-rad}}{F_P\gamma_{rad} + \gamma_{non-rad}} = F_P \frac{1 + \frac{\gamma_{rad}}{\gamma_{non-rad}}}{1 + \frac{F_P\gamma_{rad}}{\gamma_{non-rad}}} \approx F_P. \quad (3)$$

It should be emphasized that the last approximated equality in (3) is true only if $\gamma_{rad} \ll \gamma_{non-rad}$ and $F_P\gamma_{rad} \ll \gamma_{non-rad}$. If the rate of radiative transitions prevails over the rate of non-radiative transitions, then, the chemiluminescence yield is not small, and electrodynamic effects cannot significantly impact it.

Thus, the Purcell factor calculated above reflects not only an acceleration in the rate of radiation decay of excited luminol oxidation products, but also an increase in the quantum yield of metal-enhanced chemiluminescence.

Conclusions

Perforated aluminum film is a promising structure for accelerating radiation transitions and increasing the quantum yield of photo- and chemiluminescence in the visible region of the spectrum. By selecting the appropriate film thickness, radius of holes and period of their location, it is possible to adjust the structure's plasmon absorption band and acceleration maximum of radiation transitions to the desired wavelength. A thin metal film with cylindrical holes differs favorably from the metal nano-cylinder structures in that the Purcell factor, having a significant value of about 10, remains almost constant throughout the entire volume of the cylindrical hole.

Funding

This study was supported financially by grant № 23-72-00045 from the Russian Science Foundation, https://rscf.ru/project/23-72-00045/.

Conflict of interest

The authors declare that they have no conflict of interest.

References

[1] C. Dodeigne, L. Thunus, R. Lejeune. Talanta, **51** (3), 415 (2000). DOI: 10.1016/S0039-9140(99)00294-5
[2] B. Gómez-Taylor, M. Palomeque, J.V. García Mateo, J. Martínez Calatayud. J. pharmaceutical and biomedical analysis, **41** (2), 347 (2006). DOI: 10.1016/j.jpba.2005.11.040
[3] Hiroyuki Yasui, Hiromu Sakurai. Biochemical and biophysical research commun., **269** (1), 2000 (131). DOI: 10.1006/bbrc.2000.2254
[4] Wanchao Yu, Lixia Zhao. TrAC Trends in Analytical Chemistry, **136**, 116197 (2021). DOI: 10.1016/j.trac.2021.116197
[5] K. Aslan, C.D. Geddes. Chemical Society Reviews, **38** (9), 2556 (2009) DOI: 10.1039/B807498B
[6] D.R. Dadadzhanov, I.A. Gladskikh, M.A. Baranov, T.A. Vartanyan, A. Karabchevsky. Sensors and Actuators B: Chemical, **333**, 129453 (2021). DOI: 10.1016/j.snb.2021.129453
[7] D.R. Dadadzhanov, A.V. Palekhova, T.A. Vartanyan. Opt. Spectrosc., **131** (12), 1646 (2023). DOI: 10.61011/EOS.2023.12.58186.5850-23.
[8] Ashish Tiwari, S.J. Dhoble. Talanta, **180**, 1 (2018). DOI: 10.1016/j.talanta.2017.12.031
[9] Yanchun Zhao, Miao Chen, Yanan Zhang, Tao Xu, Weimin Liu. Materials Lett., **59** (1), 40 (2005). DOI: 10.1016/j.matlet.2004.09.018
[10] M. Foquet, K.T. Samiee, X. Kong, B.P. Chauduri, P.M. Lundquist, S.W. Turner, J. Freudenthal, D.B. Roitman. J. Appl. Phys., **103** (3), 034301 (2008). DOI: 10.1063/1.2831366
[11] M.J.K. Klein, M. Guillaumée, B. Wenger, L.A. Dunbar, J. Brugger, H. Heinzelmann, R. Pugin. Nanotechnology, **21** (20), 205301 (2010). DOI: 10.1088/0957-4484/21/20/205301
[12] Wang Jian, Jing Du. Appl. Sci., **6** (9), 239 (2016). DOI: 10.3390/app6090239
[13] K.M. McPeak, S.V. Jayanti, S.J.P. Kress, S. Meyer, S. Iotti, A. Rossinelli, D.J. Norris. ACS Photonics, **2** (3), 326 (2015). DOI: 10.1021/ph5004237
[14] A. Kadir, C.D. Geddes. Chemical Soc. Rev., **38** (9), 2556 (2009). DOI: 10.1039/B807498B
[15] Hao Chen, Feng Gao, Rong He, Daxiang Cui. J. colloid and interface sci., **315** (1), 158 (2007). DOI: 10.1016/j.jcis.2007.06.052

Translated by T.Zorina